Proceedings of the 2003 IEEE
International Conference on Robotics & Automation
Taipei, Taiwan, September 14-19, 2003

The Dynamic Modeling and Analysis for An Omnidirectional Mobile Robot with Three Caster Wheels

Jae Heon Chung*, Byung-Ju Yi*, Whee Kuk Kim**, Hogil Lee***

* School of Electrical Engineering and Computer Science, Hanyang University,
1271 sa-1 dong, Ansan, Kyunggi-do, Korea
(E-mail:bj@hanyang.ac.kr)
** Department of Control and Instrumentation Engineering, Korea University, Korea
*** Korea Institute of Industrial Technology, Korea

Abstract - **Recently, quite a few applications of omnidirectional mobile robots have been reported. However, understanding some fundamental issues still remains as further study. One of the issues is the exact dynamic model. Previous studies very often ignore the wheel dynamics of mobile robots and also suffer from algorithmic singularity. Thus, actuator sizing or control algorithms based on the incomplete plant model does not guarantee the control performance of the system. This paper deals with the singularity-free, exact dynamic modeling and analysis of omnidirectional mobile robot having three caster wheels. Initially, the exact dynamic model of the mobile robot including the wheel dynamics is introduced. A natural orthogonal complement approach and a singularity-free dynamic modeling approach are introduced. The joint-space and operational-space dynamic models are derived as analytical forms. Through simulation, the discrepancy of the incomplete dynamic model is shown by comparison with the exact dynamic model. Furthermore, useful aspect of operational dynamics is also discussed in terms of impact geometry.**

1. Introduction

For a mobile robot to have omni-directional characteristics on the plane, only wheels with three degrees of freedom must be employed in mobile robots. Either the caster wheel or Swedish wheel can be modeled kinematically as a three degrees-of freedom serial chain. However, it is known that either Swedish wheel or most of other type of "omni-directional wheels" are very sensitive to road conditions, and thus their operational performances are more or less limited, compared to conventional wheels. On the other hand, the active caster wheel is not sensitive to road conditions and also is able to overcome a sort of steps encountered in uneven floors by using the active driving wheel. Kinematic modeling, dynamic modeling, and numerous analyses for this type of mobile robots have been addressed recently [1-2, 6].

Campion, et. al[1] addressed the fact that the omni-directional mobile robot with three caster wheels must use more than four motors to avoid singularity, and that as admissible configuration, two motors on two of the three wheels should be used. However, their work does not provide any closed-form dynamics for omnidirectional mobile robots. Saha and Angeles [3] proposed an orthogonal complement-based dynamic model for the 2 DOF differential driven mobile robot. Yi, et.al [6] extended this methodology to a 3 DOF omnidirectional mobile robot with three caster wheels. However, this approach suffers from algorithmic singularity, depending upon the minimum coordinates for which the system dynamics is referenced or expressed. To cope with this problem, the set of minimum coordinates should be kept changed from one to another. However, this is also inconvenient and thus a singularity-free dynamic formulation is demanding.

In light of these facts, this paper introduces a singularity-free, exact dynamic model of the mobile robots including the wheel dynamics. Through simulation, the discrepancy of the incomplete dynamic model is shown by comparison with the exact dynamic model. Furthermore, useful aspect of operational dynamics is also discussed in terms of impact geometry.

2. Kinematic Modeling

Consider the mobile robot depicted in Fig. 1. This system consists of three wheels, three offset link, and a top platform. Assume that the motion of the mobile robot is constrained to the plane and there exists no sliding and skidding friction, but that rotation of the wheel about the axis vertical to the ground is allowed. XYZ represents the global reference frame, and xyz denotes a local coordinate frame attached to the mobile platform; **i**, **j**, and **k** are the unit vectors of the xyz coordinate frame. C denotes the origin of the local coordinate.

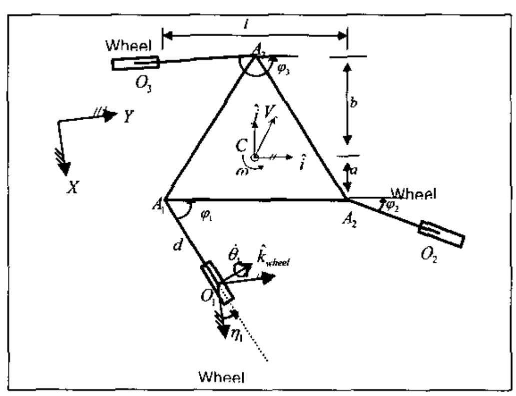

Fig. 1. Kinematics description of omnidirectional mobile robot.

We define θ as the rotating angle of the wheel and φ as the steering angle between steering link and local x-axis. η denotes the angular displacement of the wheel relative to the X-axis of the reference frame. r and d denote the radius of the wheel and the length of the steering link, respectively.

The linear velocities at the center of the wheels are given as

$$\mathbf{v}_{o1} = \dot{\theta}_1 \left(\sin\varphi_1 \mathbf{i} + \cos\varphi_1 \mathbf{j} \right) \times r\mathbf{k} \tag{1}$$

$$\mathbf{v}_{o2} = \dot{\theta}_2 \left(\sin\varphi_2 \mathbf{i} + \cos\varphi_2 \mathbf{j} \right) \times r\mathbf{k} \tag{2}$$

$$\mathbf{v}_{o3} = \dot{\theta}_3 \left(\sin\varphi_3 \mathbf{i} + \cos\varphi_3 \mathbf{j} \right) \times r\mathbf{k} \tag{3}$$

The linear velocity at C of the mobile robot can be described as

$$\begin{aligned} \mathbf{v}_c &= \mathbf{v}_{o1} + \dot{\eta}_1 \mathbf{k} \times \overline{O_1 A_1} + \omega \mathbf{k} \times \overline{A_1 C} \\ &= \dot{\theta}_1 \left(\sin\varphi_1 \mathbf{i} + \cos\varphi_1 \mathbf{j} \right) \times r\mathbf{k} \\ &\quad + \dot{\eta}_1 \mathbf{k} \times \left(-d\cos\varphi_1 \mathbf{i} + d\sin\varphi_1 \mathbf{j} + h\mathbf{k} \right) \\ &\quad + \omega \mathbf{k} \times \left(\frac{l}{2}\mathbf{i} + a\mathbf{j} \right) \end{aligned} \tag{4}$$

$$\begin{aligned} \mathbf{v}_c &= \mathbf{v}_{o2} + \dot{\eta}_2 \mathbf{k} \times \overline{O_2 A_2} + \omega \mathbf{k} \times \overline{A_2 C} \\ &= \dot{\theta}_2 \left(\sin\varphi_2 \mathbf{i} + \cos\varphi_2 \mathbf{j} \right) \times r\mathbf{k} \\ &\quad + \dot{\eta}_2 \mathbf{k} \times \left(-d\cos\varphi_2 \mathbf{i} + d\sin\varphi_2 \mathbf{j} + h\mathbf{k} \right) \\ &\quad + \omega \mathbf{k} \times \left(-\frac{l}{2}\mathbf{i} + a\mathbf{j} \right) \end{aligned} \tag{5}$$

$$\begin{aligned} \mathbf{v}_c &= \mathbf{v}_{o3} + \dot{\eta}_3 \mathbf{k} \times \overline{O_3 A_3} + \omega \mathbf{k} \times \overline{A_3 C} \\ &= \dot{\theta}_3 \left(\sin\varphi_3 \mathbf{i} + \cos\varphi_3 \mathbf{j} \right) \times r\mathbf{k} \\ &\quad + \dot{\eta}_3 \mathbf{k} \times \left(-d\cos\varphi_3 \mathbf{i} + d\sin\varphi_3 \mathbf{j} + h\mathbf{k} \right) + \omega \mathbf{k} \times (\text{-b}\mathbf{j}) \end{aligned} \tag{6}$$

where ω representing the angular velocity of the mobile platform can be described as

$$\omega = \dot{\eta}_1 + \dot{\varphi}_1 \tag{7}$$

$$\omega = \dot{\eta}_2 + \dot{\varphi}_2 \tag{8}$$

$$\omega = \dot{\eta}_2 + \dot{\varphi}_2 \tag{9}$$

$\mathbf{v}_c = \begin{bmatrix} v_{cx} & v_{cy} \end{bmatrix}^T$ of Eqs. (4)-(6) and ω of Eqs. (7)-(9) can be expressed as one matrix form given by

$$\begin{bmatrix} v_{cx} \\ v_{cy} \\ \omega \end{bmatrix} = \begin{bmatrix} -d\sin\varphi_1 - a & r\cos\varphi_1 & -a \\ -d\cos\varphi_1 + l/2 & -r\sin\varphi_1 & l/2 \\ 1 & 0 & 1 \end{bmatrix} \begin{bmatrix} \dot{\eta}_1 \\ \dot{\theta}_1 \\ \dot{\varphi}_1 \end{bmatrix} \tag{10}$$

$$\begin{bmatrix} v_{cx} \\ v_{cy} \\ \omega \end{bmatrix} = \begin{bmatrix} -d\sin\varphi_2 - a & r\cos\varphi_2 & -a \\ -d\cos\varphi_2 - l/2 & -r\sin\varphi_2 & -l/2 \\ 1 & 0 & 1 \end{bmatrix} \begin{bmatrix} \dot{\eta}_2 \\ \dot{\theta}_2 \\ \dot{\varphi}_2 \end{bmatrix} \tag{11}$$

$$\begin{bmatrix} v_{cx} \\ v_{cy} \\ \omega \end{bmatrix} = \begin{bmatrix} -d\sin\varphi_3 + b & r\cos\varphi_3 & b \\ -d\cos\varphi_3 & -r\sin\varphi_3 & 0 \\ 1 & 0 & 1 \end{bmatrix} \begin{bmatrix} \dot{\eta}_3 \\ \dot{\theta}_3 \\ \dot{\varphi}_3 \end{bmatrix} \tag{12}$$

From (10) through (12), the mobile robot can be visualized as a parallel mechanism. The variable (η) interfacing the wheel to the ground enables this model. Thus, the kinematics of the mobile robot is instantaneously equivalent to that of typical parallel robot that is connected to a fixed ground.

The intermediate coordinate transfer method, which was popularly employed in parallel robot community, will be employed to derive the forward kinematic relation. Taking the inverses of Eqs. (10)-(12), we have

$$\begin{bmatrix} \dot{\eta}_1 \\ \dot{\theta}_1 \\ \dot{\varphi}_1 \end{bmatrix} = \frac{1}{dr} \begin{bmatrix} -r\sin\varphi_1 & -r\cos\varphi_1 & \frac{l}{2} r\cos\varphi_1 - ar\sin\varphi_1 \\ d\cos\varphi_1 & -d\sin\varphi_1 & \frac{l}{2} d\sin\varphi_1 + ad\cos\varphi_1 \\ r\sin\varphi_1 & r\cos\varphi_1 & dr + ar\sin\varphi_1 - \frac{l}{2} r\cos\varphi_1 \end{bmatrix} \dot{\mathbf{u}} \tag{13}$$

$$\begin{bmatrix} \dot{\eta}_2 \\ \dot{\theta}_2 \\ \dot{\varphi}_2 \end{bmatrix} = \frac{1}{dr} \begin{bmatrix} -r\sin\varphi_2 & -r\cos\varphi_2 & \frac{l}{2} r\cos\varphi_2 - ar\sin\varphi_2 \\ d\cos\varphi_2 & -d\sin\varphi_2 & -\frac{l}{2} d\sin\varphi_2 + ad\cos\varphi_2 \\ r\sin\varphi_2 & r\cos\varphi_2 & dr + ar\sin\varphi_2 + \frac{l}{2} r\cos\varphi_2 \end{bmatrix} \dot{\mathbf{u}} \tag{14}$$

$$\begin{bmatrix} \dot{\eta}_3 \\ \dot{\theta}_3 \\ \dot{\varphi}_3 \end{bmatrix} = \frac{1}{dr} \begin{bmatrix} -r\sin\varphi_3 & -r\cos\varphi_3 & br\sin\varphi_3 \\ d\cos\varphi_3 & -d\sin\varphi_3 & -bd\cos\varphi_3 \\ r\sin\varphi_3 & r\cos\varphi_3 & dr - br\sin\varphi_3 \end{bmatrix} \dot{\mathbf{u}} \tag{15}$$

The second-order kinematic influence coefficient, which denotes the variation of the Jacobian with respect to the joint angle, is expressed as

$$\left[{}_i\boldsymbol{H}^u_{\phi\phi} \right] = \frac{\partial}{\partial \phi} \left(\left[{}_i\boldsymbol{G}^u_{\phi} \right] \right) \tag{16}$$

$$\left[{}_i\boldsymbol{H}^{\phi}_{uu} \right] = -\left[{}_i\boldsymbol{G}^{\phi}_u \right]^T \left(\left[{}_i\boldsymbol{G}^{\phi}_u \right] \circ \left[{}_i\boldsymbol{H}^u_{\phi\phi} \right] \right) \left[{}_i\boldsymbol{G}^{\phi}_u \right] \tag{17}$$

where the Hessian $\left[{}_i\boldsymbol{H}^u_{\phi\phi} \right]$ describes that it affect the velocity of the operational space set (**u**) on the acceleration of the i th chain joint variable and it has $M \times N \times N$ dimension. M and N denote the number of the output and the number of the input joints, respectively. $\left[{}_iH^{\phi}_{uu} \right]$ denotes the inverse of $\left[{}_iH^u_{\phi\phi} \right]$. The operator '∘', called Generalized Dot Product [7], is employed to simplify the final form of this second-order inverse kinematic model.

Since the omnidirectional mobile robot has mobility 3, we can define three minimum (or independent) coordinates. Let ϕ_a be the independent input vector consisting of three independent joint variables such as two driving variables $(\dot{\theta}_1, \dot{\theta}_2)$ and one steering variable $(\dot{\varphi}_3)$. Then, the velocity relationship between the output and the independent joint variables of the mobile robot can be obtained as

$$\dot{\underline{\phi}}_a = \left[\boldsymbol{G}^a_u \right] \dot{\underline{u}} \tag{18}$$

$$\ddot{\underline{\phi}}_a = \left[\boldsymbol{G}^a_u \right] \ddot{\underline{u}} + \dot{\underline{u}}^T \left[\boldsymbol{H}^a_{uu} \right] \dot{\underline{u}} \tag{19}$$

where

$$\left[\boldsymbol{G}^a_u \right] = \left[\left[{}_1\boldsymbol{G}^{\phi}_u \right]^T_{2;} \quad \left[{}_2\boldsymbol{G}^{\phi}_u \right]^T_{2;} \quad \left[{}_3\boldsymbol{G}^{\phi}_u \right]^T_{3;} \right]^T \tag{20}$$

$$\left[\boldsymbol{H}_{uu}^{a}\right]=\begin{bmatrix}\left[{}_{1}\boldsymbol{H}_{uu}^{\phi}\right]_{2::}\\\left[{}_{2}\boldsymbol{H}_{uu}^{\phi}\right]_{2::}\\\left[{}_{3}\boldsymbol{H}_{uu}^{\phi}\right]_{3::}\end{bmatrix} \tag{21}$$

$\left[\boldsymbol{G}_{u}^{a}\right]$ represents the inverse Jacobian matrix of the mobile robot and the Hessian matrix $\left[\boldsymbol{H}_{uu}^{a}\right]$ affect the velocity of the independent coordinate set($\underline{\phi}_a$) on the acceleration of the operational space.

$\left[{}_{i}\boldsymbol{G}_{u}^{\phi}\right]_{j:}$ and $\left[{}_{i}\boldsymbol{H}_{uu}^{\phi}\right]_{j::}$ denote the j th row of the Jacobian and the j th plane of the Hessian matrix at the i th chain, respectively. The planes of $\left[\boldsymbol{H}_{uu}^{a}\right]$ are composed of planes of $\left[{}_{i}\boldsymbol{H}_{uu}^{\phi}\right]$, which correspond to the independent joint set[7].

3. Dynamic Modeling

Two approaches will be introduced to derive the dynamic model of the omnidirectional mobile robot with three caster wheels.

3.1 The natural orthogonal complement algorithm

Saha and Angeles [3] employed the concept of orthogonal complement [3] using the matrix of nonholonomic constraints to develop the dynamic equations of the 2 DOF mobile robot. Yi, et.al [6] extended this concept to derive the dynamic model of an omnidirectional mobile robot with three caster wheels.

This method converts the dynamic model derived in terms of Lagrangian coordinates into that in terms of minimum coordinates by embedding nonholonomic constraints. During the process of the dynamic modeling, it is necessary to obtain the internal kinematic relation between the independent (or minimum) coordinates ($\underline{\dot{\phi}}_a$) and the dependent coordinates ($\underline{\dot{\phi}}_p$). It is given by

$$J_p\underline{\dot{\phi}}_p = J_a\underline{\dot{\phi}}_a \tag{22}$$

where J_p is always given a square matrix. Then, the mapping relation between $\underline{\dot{\phi}}_p$ and $\underline{\dot{\phi}}_a$ is expressed as

$$\underline{\dot{\phi}}_p = J_p^{-1}J_a\underline{\dot{\phi}}_a \tag{23}$$

where the invertibility of J_p is associated with singularity.

The velocity of each individual body can be written as a linear transformation $\left(G_p, G_a\right)$ of all joint rates and the congregation of the twists of all rigid-bodies can be denoted as a generalized twist, given by

$$\underline{t} = G_p\underline{\dot{\phi}}_p + G_a\underline{\dot{\phi}}_a \tag{24}$$

where $\underline{t}=\left[\underline{t}_1^T,\ldots,\underline{t}_7^T\right]$. Substituting the relation given in (23) into (24), the generalized twist $(\underline{t})$ can be written in terms of the independent joint rates $\left(\underline{\dot{\phi}}_a\right)$ as

$$\underline{t} = G\underline{\dot{\phi}}_a \tag{25}$$

where $G = G_a + G_pJ_p^{-1}J_a$.

Now, the nonholonomic constraint given by G will be embedded into the system dynamics given in terms of the Lagrangian coordinates. Then, the final form of dynamic relation is expressed as [4]

$$G^TMG\underline{\ddot{\phi}}_a = -G^T\left(M\dot{G}+WMG\right)\underline{\dot{\phi}}_a + \underline{\tau} \tag{26}$$

where M denotes the block-diagonal, extended mass matrix and $\underline{\tau}$ denotes the joint torque vector. Re-ordering (26) yields the dynamic model in terms of the independent coordinates:

$$\underline{\tau} = I\left(\underline{\phi}\right)\underline{\ddot{\phi}}_a + C\left(\underline{\phi},\underline{\dot{\phi}}_a\right)\underline{\dot{\phi}}_a \tag{27}$$

where $\phi = \left[\phi_a, \phi_p\right]$.

The shortcoming of this algorithm comes from the inversion of J_p in (23). Yi and Kim [8] addressed that an algorithmic singularity would happen in the omnidirectional mobile robot with three caster wheels, when the reciprocal screws of the three independent joints meets at one position or meets at infinity. It is found from (26) that this kinematic singularity propagates to dynamics since it requires the inversion of J_p. To cope with this problem, the set of independent coordinates should be kept changed to get away from the singularity. However, it is inconvenient. Thus, the natural orthogonal complement algorithm cannot be employed as a dynamic modeling approach stably.

3.2 Lagrange's form of D'Alembert principle

A dynamic modeling approach employing Lagrange's form of D'Alembert principle will be employed to resolve the singularity problem. To derive the dynamic model of this system, we convert the system into an open-tree structure. Cutting joints of close chains make the open tree structure. Initially, by using the Lagrangian dynamic formulation, a dynamic model of each serial chain is evaluated. Next, by using the virtual work, the open chain dynamics can be directly incorporated into closed chain dynamics (for instance, joint-space dynamics or operational-space dynamics).

Cutting joints of closed chains makes the open tree structure. As shown in Fig. 2, the system at hand consists of seven rigid bodies. Each rigid body has its kinetic energy. Thus, initially we use the Lagrangian formulation that is an "energy-based" approach to dynamics. The kinetic energy of i th rigid body, k_i can be expressed as

$$k_i = \frac{1}{2}m_iv_{C_i}^Tv_{C_i} + \frac{1}{2}{}^i\omega_i^T\,{}^{C_i}I_i\,{}^i\omega_i \tag{28}$$

where the first term is the kinetic energy due to the linear velocity at the center of the mass of the rigid body, and the second term is the kinetic energy due to the angular velocity of the rigid body. Also m_i and ${}^{ci}I_i$ are mass and inertia matrix of the i th link, respectively. The total kinetic energy of the open chain is the sum of the kinetic energies of all rigid bodies.

$$k = \sum_{i=1}^{n} k_i \tag{29}$$

The Lagrangian dynamic formulation is described as

$$L(\theta,\dot{\theta}) = k(\theta,\dot{\theta}) - u(\theta) \tag{30}$$

$$\frac{d}{dt}\frac{\partial k}{\partial \dot{\theta}} - \frac{\partial k}{\partial \theta} = \underline{\tau} \tag{31}$$

where $\underline{\tau}$ is the n x 1 vector joint torques. Since we assume that the mobile robot moves only in the planar domain, the potential energy is ignored.

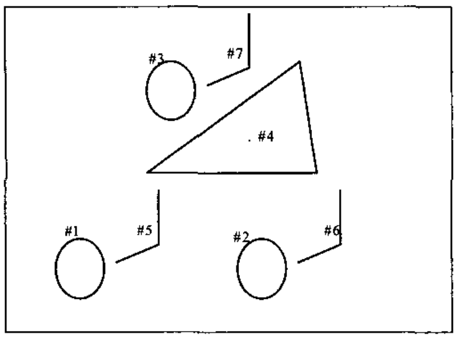

Fig. 2. Disassembled mobile robot

The linear velocity and angular velocity at the center of each wheel (1, 2, and 3) are described as

$${}^{i}v_{c_1} = r(\cos\varphi_i \mathbf{i} - \sin\varphi_i \mathbf{j})\dot{\theta}_i \tag{32}$$

$${}^{i}\omega_{c_1} = \dot{\eta}_i \mathbf{k} + \dot{\theta}_i(\sin\varphi_i \mathbf{i} + \cos\varphi_i \mathbf{j}) \tag{33}$$

And the linear velocity and angular velocity at the center of each offset link (5, 6, and 7) are described as

$${}^{i}v_{c2} = v_{O_i} + \dot{\eta}_i \mathrm{k} \times (-p\cos\varphi_i \mathbf{i} + p\sin\varphi_i \mathbf{j}) \tag{34}$$

$${}^{i}\omega_{c_2} = \dot{\eta}_i \mathbf{k} \tag{35}$$

The kinetic energies of the wheel and the offset link of the i th chain are expressed as

$${}^{i}k_1 = \frac{1}{2} m_1 {}^{i}v_{c_1}^{\ T}\, {}^{i}v_{c_1} + \frac{1}{2} {}^{i}\omega_{c_1}^{\ T}\, {}^{i}I_1 {}^{i}\omega_{c_1} \tag{36}$$

$${}^{i}k_2 = \frac{1}{2} m_2 {}^{i}v_{c_2}^{\ T}\, {}^{i}v_{c_2} + \frac{1}{2} {}^{i}\omega_{c_2}^{\ T}\, {}^{i}I_2 {}^{i}\omega_{c_2} \tag{37}$$

Then, the total kinetic energy of the i th chain is

$${}^{i}k = {}^{i}k_1 + {}^{i}k_2 \tag{38}$$

Now, substituting (38) into (31) yield an open chain dynamics of the i th chain as [7]

$${}_{i}\mathbf{T}_{\phi} = \left[{}_{i}I^{*}_{\phi\phi}\right]{}_{i}\ddot{\underline{\phi}} + {}_{i}\dot{\underline{\phi}}^{T}\left[{}_{i}P^{*}_{\phi\phi\phi}\right]{}_{i}\dot{\underline{\phi}} - {}_{i}T_{ext} \tag{39}$$

where

$$\left[{}_{i}I^{*}_{\phi\phi}\right] = \begin{bmatrix} m_2 p^2 + {}^{i}I_{z1} + {}^{i}I_{z2} & 0 & 0 \\ 0 & \frac{3}{2} m_1 r^2 + m_2 r^2 & 0 \\ 0 & 0 & 0 \end{bmatrix} \tag{40}$$

$${}_{i}T_{ext} = \left(\overline{O_i A_i} - r\mathbf{k}\right) \times {}_{i}F_{ext} \tag{41}$$

$\left[{}_{i}I^{*}_{\phi\phi}\right]$ and $\left[{}_{i}P^{*}_{\phi\phi\phi}\right]$ denote the inertia matrix and the inertia power array referenced to the Lagrangian coordinate set, respectively. $\left[{}_{i}P^{*}_{\phi\phi\phi}\right]$, which reflects the change of $\left[{}_{i}I^{*}_{\phi\phi}\right]$, is given a zero matrix since $\left[{}_{i}I^{*}_{\phi\phi}\right]$ is given constant. ${}_{i}F_{ext}$ denotes the vector sum of the external forces along the lateral and longitudinal directions, which is exerted at the contact point between the wheel of the ith chain and the ground.

3.3 Operational-space dynamics

By using the virtual work principle, the operational space dynamic model can be directly obtained from the dynamics in terms of Lagrangian coordinate (${}_{i}\underline{\phi}$) set, according to

$$\mathbf{T}_u \cdot \delta u = \sum_{i}^{3} {}_{i}\mathbf{T}_{\phi}\, \delta\, {}_{i}\phi \tag{42}$$

where $\mathbf{T}_u$ and ${}_{i}\mathbf{T}_{\phi}$ denote the operational force vector and the effective joint torque vector of the i th chain, respectively. Eq. (42) can be converted as

$$\mathbf{T}_u = \sum_{i=1}^{3} \left[{}_{i}G^{\phi}_{u}\right] {}_{i}\mathbf{T}_{\phi} + \mathbf{T}_{pl} \tag{43}$$

by employing a kinematic relation, which relates the Lagrangian coordinate set (${}_{i}\underline{\phi}$) to the operational space coordinate set($\mathbf{u}$) of the given mobile robot. $\mathbf{T}_{pl}$ denotes the operational force vector applied to the platform.

Now, by substituting the open chain dynamics of the three chains into Eq. (43), the operational space dynamic model is derived as [7]

$$\mathbf{T}_u = \left[I^{*}_{uu}\right]\ddot{\underline{u}} + \dot{\underline{u}}^{T}\left[P^{*}_{uuu}\right]\dot{\underline{u}} - F_{ext} \tag{44}$$

where denote the inertia matrix $\left[I^{*}_{uu}\right]$ and the inertia power array $\left[P^{*}_{uuu}\right]$ referenced to the operational space coordinate set($\mathbf{u}$) are given by

$$\left[I^{*}_{uu}\right] = \sum_{i=1}^{3} \left[{}_{i}G^{\phi}_{u}\right]^{T} \left[{}_{i}I^{*}_{\phi\phi}\right]\left[{}_{i}G^{\phi}_{u}\right] + \left[{}_{pl}I^{*}_{uu}\right] \tag{45}$$

$$\left[P^{*}_{uuu}\right] = \sum_{i=1}^{3}\left[\left[{}_{i}G^{\phi}_{u}\right]^{T}\left[\left[{}_{i}G^{\phi}_{u}\right]^{T} \circ \left[{}_{i}P^{*}_{\phi\phi\phi}\right] - \left[{}_{i}I^{*}_{uu}\right] \circ \left[{}_{i}H^{u}_{\phi\phi}\right]\right]\left[{}_{i}G^{\phi}_{u}\right]\right] + \left[{}_{pl}P^{*}_{uuu}\right] \tag{46}$$

with

$$\left[{}_{pl}I^{*}_{uu}\right] = \begin{bmatrix} m_{pl} & 0 & 0 \\ 0 & m_{pl} & 0 \\ 0 & 0 & \frac{1}{2} m_{pl} R^2 \end{bmatrix} \tag{47}$$

$$\left[{}_{i}I^{*}_{uu}\right] = \left[{}_{i}G^{\phi}_{u}\right]^{T}\left[{}_{i}I^{*}_{\phi\phi}\right]\left[{}_{i}G^{\phi}_{u}\right] \tag{48}$$

$$F_{ext} = \sum_{i=1}^{3} \left[{}_{i}G^{\phi}_{u}\right]^{T} {}_{i}T_{ext} \tag{49}$$

Each of the first term of Eq. (45) and Eq. (46) comes from each open chain dynamics, and the second terms, $\left[{}_{pl}\boldsymbol{I}^{*}_{uu}\right]$ and $\left[{}_{pl}\boldsymbol{P}^{*}_{uuu}\right]$, denote the inertia matrix and the inertia power array of the platform, respectively. In Eq. (47), m_{pl} and R represent the mass and the radius of the top platform, respectively.

As shown in Eq. (46), the operational-space dynamic formulation also uses the matrix inversion $\left[{}_{i}\boldsymbol{G}^{\phi}_{u}\right]$ that corresponds to the inverse Jacobian of each chain (Eq. (13) through (15)). Note that the inverse relations are not singular unless the offset distance or the radius of the wheel is zero[2]. Thus, the dynamic modeling approach based on Lagrange's form of D'Alembert principle is singularity-free in comparison to orthogonal complement based algorithm [6].

3.4 Independent joint-space dynamics

The dynamic model referenced to the independent coordinates ($\underline{\phi}_a$) can be also obtained by using virtual work principal. The total system dynamic model can be directly obtained from the operational space dynamics according to

$$\mathbf{T}_a \cdot \delta\phi_a = \mathbf{T}_u \cdot \delta u \tag{50}$$

Eq. (50) can be converted as

$$\mathbf{T}_a = \left[\boldsymbol{G}^{u}_{a}\right]^{T}\mathbf{T}_u \tag{51}$$

by using the kinematics model, which relates the operational space coordinate set(**u**) to the independent coordinate set ($\underline{\phi}_a$) of the given mechanism.

Now, the dynamic model expressed in terms of a minimum set of coordinate ($\underline{\phi}_a$) is obtained as

$$\mathbf{T}_a = \left[\boldsymbol{I}^{*}_{aa}\right]\ddot{\underline{\phi}}_a + \dot{\underline{\phi}}_a^{T}\left[\boldsymbol{P}^{*}_{aaa}\right]\dot{\underline{\phi}}_a \tag{52}$$

by substituting the operational space dynamics given in Eq. (44) into (51), where $\left[\boldsymbol{I}^{*}_{aa}\right]$ and $\left[\boldsymbol{P}^{*}_{aaa}\right]$ given by

$$\left[\boldsymbol{I}^{*}_{aa}\right] = \left[\boldsymbol{G}^{u}_{a}\right]^{T}\left[\boldsymbol{I}^{*}_{uu}\right]\left[\boldsymbol{G}^{u}_{a}\right] \tag{53}$$

$$\left[\boldsymbol{P}^{*}_{aaa}\right] = \left[\left[\boldsymbol{G}^{u}_{a}\right]^{T}\left\{\left[\boldsymbol{G}^{u}_{a}\right]^{T}\circ\left[\boldsymbol{P}^{*}_{uuu}\right] - \left[\boldsymbol{I}^{*}_{uu}\right]\circ\left[\boldsymbol{H}^{a}_{uu}\right]\right\}\left[\boldsymbol{G}^{u}_{a}\right]\right] \tag{54}$$

denotes the inertia matrix and the inertia power array referenced to the independent coordinate set($\underline{\phi}_a$), respectively.

4. Impulse Modeling

The exact dynamic model in terms of the operational space can be employed to derive the impulse model when a mobile robot collides with external environment.

Most generally, the impact is partially elastic in the range of $0<e<1$. When the coefficient of restitution e is known, the velocity of colliding bodies can be obtained immediately after the impact. The component of the increment of relative velocity along a vector $\boldsymbol{n}$ that is normal to the contact surface is given by [4]

$$\left(\Delta v_1 - \Delta v_2\right)^{T}\boldsymbol{n} = -(1+e)\left(v_1 - v_2\right)^{T}\boldsymbol{n} \tag{55}$$

where v_1 and v_2 are the absolute velocities of the colliding bodies immediately before impact and Δv_1 and Δv_2 are the velocity increments immediately after impact.

The external impact modeling methodology for serial type system is introduced by Walker[8]. When a robot system interacts with environment, the dynamic model of general robot systems is given as

$$\mathbf{T}_u = \left[\boldsymbol{I}^{*}_{uu}\right]\ddot{\underline{u}} + \dot{\underline{u}}^{T}\left[\boldsymbol{P}^{*}_{uuu}\right]\dot{\underline{u}} - \boldsymbol{F}_{ext} \tag{56}$$

where is $\boldsymbol{F}_{ext}$ the impulsive external force at the contact point.

Integration of the dynamic model given in Eq(56) over contacting time interval gives

$$\int_{t_0}^{t_0+\Delta t}\mathbf{T}_u dt = \int_{t_0}^{t_0+\Delta t}\left[\boldsymbol{I}^{*}_{uu}\right]\ddot{\underline{u}}dt + \int_{t_0}^{t_0+\Delta t}\dot{\underline{u}}^{T}\left[\boldsymbol{P}^{*}_{uuu}\right]\dot{\underline{u}}dt - \int_{t_0}^{t_0+\Delta t}\boldsymbol{F}_{ext}dt \tag{57}$$

Since the position and velocities are assumed finite all the time during impact, the integral term involving $\dot{\underline{u}}^{T}\left[\boldsymbol{P}^{*}_{uuu}\right]\dot{\underline{u}}$ becomes zero as Δt goes to zero, as does the term involving actuation input $\mathbf{T}_u$. Thus, we obtain the following, simple expression

$$\left[\boldsymbol{I}^{*}_{uu}\right]\left(\dot{\underline{u}}(t+\Delta t) - \dot{\underline{u}}(t)\right) = \hat{\boldsymbol{F}}_{ext} \tag{58}$$

where $\hat{\boldsymbol{F}}_{ext} = \int_{t_0}^{t_0+\Delta t}\boldsymbol{F}_{ext}dt$ is defined as the external impulse at the contact point. Thus, the velocity increment at the contact point is

$$\Delta\dot{\underline{u}} = \left[\boldsymbol{I}^{*}_{uu}\right]^{-1}\hat{\boldsymbol{F}}_{ext} \tag{59}$$

Assuming that the robot impacts on a fixed solid surface, substitution of Eq.(59) into Eq.(55) gives

$$\left(\left[\boldsymbol{I}^{*}_{uu}\right]^{-1}\hat{\boldsymbol{F}}_{ext}\right)^{T}\boldsymbol{n} = -(1+e)\left(\dot{\underline{u}}\right)^{T}\boldsymbol{n} \tag{60}$$

Since the absolute velocity (v_1) with respect to platform coordinate is given $\dot{\underline{u}}$ and the velocity increment of the fixed surface is always zero$(v_2 = \Delta v_2 = 0)$. Impulse always acts at the contact point in the direction of the surface normal vector $\boldsymbol{n}$ under the assumption that no friction exits on the contacting surface. Thus, we have

$$\hat{\boldsymbol{F}}_{ext} = \hat{F}_{ext}\boldsymbol{n} \tag{61}$$

Substituting Eq.(61) into Eq.(60), we derive the magnitude of the external impulse as follows

$$\hat{F}_{ext} = \frac{-(1+e)\dot{\underline{u}}^{T}\boldsymbol{n}}{\boldsymbol{n}^{T}\left[\boldsymbol{I}^{*}_{uu}\right]^{-1}\boldsymbol{n}}. \tag{62}$$

5. Simulation

In order to verify the benefit of the exact dynamic model of the mobile robot, several simulations were carried out. We employ the parameters given in Table 1.

The mobile robot travels along the circular path given in Fig. 3 (a). It rotates in the counterclockwise direction. The initial and final positions are the same, and the initial and final velocities are given zero. The radius of the circle is R. β denoting the angle between the global

X-axis and the local unit vector **i** is given as a fifth-order polynomial, such as

$$\beta(t) = a_0 + a_1 t + a_2 t^2 + a_3 t^3 + a_4 t^4 + a_5 t^5 \tag{63}$$

For the given initial conditions, we have

$$a_0 = 0, \quad a_1 = 0, \quad a_2 = 0, \quad a_3 = 20\pi / 60^3$$

$$a_4 = -30\pi / 60^4, \quad a_5 = 12\pi / 60^5$$

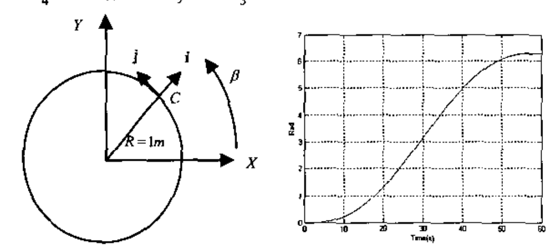

(a) (b)

Fig. 3. Trajectory of the mobile robot

Table 1. Parameters

Link	l	r	d	a	b	h
[m]	0.173	0.025	0.025	0.05	0.1	0.045
Mass	Wheel		Link		Platform	
[kg]	0.5		0.05		5	
Inertia tensor	[kg·m²] $(i = 1,2,3)$					
Wheel[I_i]	$diag[0.7813 \quad 1.5625 \quad 0.7813]*10^{-4}$					
Offset link[I_i]	$diag[8.438 \quad 11.042 \quad 2.604]*10^{-6}$					

Previous studies very often ignore the wheel dynamics of mobile robots. Thus, actuator sizing or control algorithms based on the incomplete plant model can not guarantee the control performance of the system. Based on the singularity-free, exact dynamic modeling derived in this paper, we would like to show the discrepancy of the incomplete dynamic model by comparison with the exact dynamic model.

Among the operational space based dynamic models, the characteristic of the inertia matrix $\left[I_{uu}^{*}\right]$ will be compared. Specifically, during the circular motion of the mobile robot, it keeps the original configuration with respect to the body-fixed coordinate frame. Thus, the dynamic model maintains the same value. When we compare the content of the inertia matrix of the incomplete dynamic model, given by

$$\left[I_{uu}^{*}\right] = \begin{bmatrix} 5 & 0 & 0 \\ 0 & 5 & 0 \\ 0 & 0 & 0.025 \end{bmatrix}$$

with that of the proposed, exact dynamic model including the wheel dynamics, given by

$$\left[I_{uu}^{*}\right] = \begin{bmatrix} 5.4329 & 0.0537 & -0.00078 \\ 0.0537 & 7.5379 & 0.0107 \\ -0.00078 & 0.0107 & 0.0397 \end{bmatrix}$$

there exists some offset between the two models. The discrepancy is severe especially in the y-direction, even though it will have different result depending upon the configuration of the mobile robot.

Another observation can be made by comparing the operational forces, given in (43), for the two cases. As shown in Fig. 4 through Fig. 7, there are significant errors at F_x and F_y between the two models. This fact tells us that when employing incomplete dynamic model, the required control performance of some dynamic model-based control algorithms will deteriorate.

The exact dynamic model of the mobile robot also enables one to investigate the impact geometry of the mobile system.

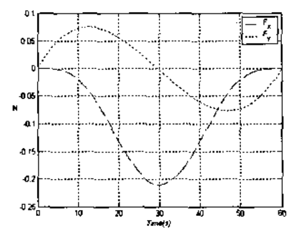

Fig. 4. X and Y directional operational forces with wheel dynamics

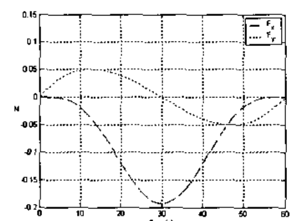

Fig. 5. X and Y directional operational forces without wheel dynamics

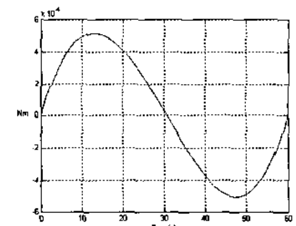

Fig. 6. Z-directional operational moment with wheel dynamics

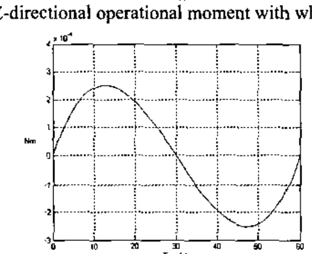

Fig. 7. Z-directional operational moment without wheel dynamics

The impulse characteristic of the mobile robot can be studied by analyzing the ellipse geometry. For this, the external impulse measure given in terms of the operational space will be employed. We assume that the coefficient of restitution e is 0.8 and the velocity of the origin of the local coordinate is given $1m/s$. The ellipses of Fig. 8 through Fig. 11 show the configurations $(\varphi_1, \varphi_2, \varphi_3)$ of each mobile robot and their corresponding impulse geometries. The ellipses denote the amount of normalized impulse that may be experienced when the mobile robot tends to move from the current configuration to every direction. It is observed that the amount of impulse is greater in the moving direction as compared to that of the other directions. Turning configuration given in Fig. 10 shows a uniform ellipsoid since the wheel dynamics contributes to the impulse geometry symmetrically. On the other hand, ignoring the wheel dynamics will always generate a circular shape. In this sense, exact dynamic model also contributes to analysis of the impact geometry.

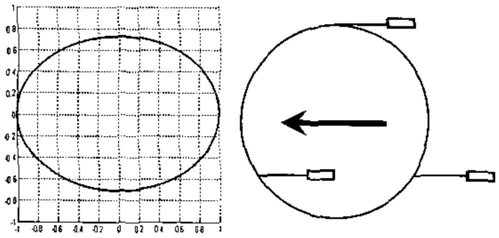

(a)Ellipse (b)Mobile configuration

Fig. 8. Steering angle $(0^\circ, 0^\circ, 0^\circ)$

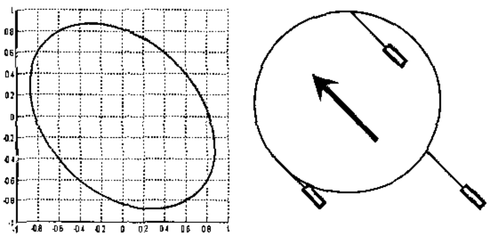

(a)Ellipse (b)Mobile configuration

Fig. 9. Steering angle $(45^\circ, 45^\circ, 45^\circ)$

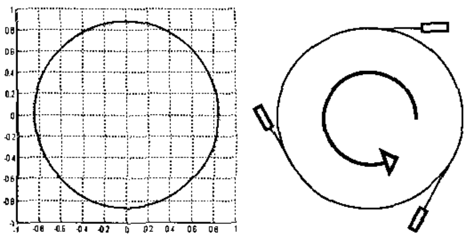

(a)Ellipse (b)Mobile configuration

Fig. 10. Steering angle $(240^\circ, 120^\circ, 0^\circ)$

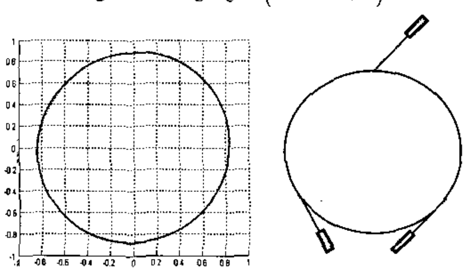

(a)Ellipse (b)Mobile configuration

Fig. 11. Steering angle $(60^\circ, 135^\circ, 315^\circ)$

5. Conclusion

In this paper, we derive the kinematics and the exact dynamic model for an omnidirectional mobile robot having three caster wheels. Singularity-free dynamic models for both operational space and independent-joint space are derived. It is shown through simulation that the operational-based dynamic model including the wheel dynamics is of significance to make sure the operational performances of dynamic model-based control algorithms, and it is also useful in the impact analysis when the mobile robot collides with some dynamic environments.

References

[1] C. Campion, G. Batin, and B. D'Andrea-Novel, "Structural Properties and Classification of Kinematics and Dynamics Models of Wheeled Mobile Robot", IEEE Trans. on Robot and Automation, Vol. 4, No. 2, 1987, pp. 281-340.

[2] B.-J. Yi and W.K. Kim, "The Kinematics for Redundantly Actuated Omni-directional Mobile Robots", Journal of Robotic Systems 19(6), 2002, pp. 255-267.

[3] S.K. Saha and J. Angels, "Kinematics and Dynamics of a Three Wheeled 2-DOF AVG", IEEE Int'l Conf. On Robotics and Automation, 1989, pp. 1572-1577.

[4] J. Wittenburg, Dynamics of systems of rigid bodies, Stuttgart, B.G. Teubner, 1977.

[5] M. Thomas, M. Yuan-Chou, and D. Tesar, "Optimal Actuator Sizing for Robotic Manipulators Based on Local Dynamic Criteria", ASME J. Mech., Trans. Automat. Design, Vol. 107, 1985, pp. 163-169.

[6] B.-J. Yi, W. K. Kim, and S. Park, "Kinematic/Dynamic Modeling and Analysis of Omni-directional Mobile Robots with Redundant Actuation", Tutorial(TS2) for vehicle mechanisms having actuation redundancy and adaptable kinematic structure, IEEE/RSJ Int'l Conf. on Intelligent Robots and Systems, 1999, pp. 1-25.

[7] R.A. Freeman and D. Tesar, "Dynamic Modeling of Serial and Parallel Mechanisms/Robotic Systems," Part I-Methodology, Part II-Applications, 20th ASME Biennial Mechanism Conf., Orlando, FL,1988, pp. 7-27.

[8] I. D. Walker, "The use of kinematic redundancy in reducing impact and contact effects in manipulation", IEEE Int'l Conf. on Robotics and Automation, 1990, pp. 434-439.

[9] S.H. Lee, B.-J. Yi, S.H. Kim, and Y.K. Kwak, "Modeling and analysis of internal impact for general classes of robotic mechanism", IEEE/RSJ Int'l Conf. on Intelligent Robots and Systems, 2000, pp. 1955-1962.